Inorg. Chem. **2006**, *45*, 3369–3377

Syntheses and Molecular Structure of Some Rh and Ru Complexes with the Chelating Diphenyl (2-Pyridyl)phosphine Ligand

Katarzyna Wajda-Hermanowicz,* Zbigniew Ciunik, and Andrzej Kochel

Faculty of Chemistry, University of Wrocław, 14 Joliot-Curie Street, 50-383 Wrocław, Poland

Received August 24, 2005

The rhodium(III) complex *mer,cis*-[$RhCl_3$(PPh_2py-*P,N*)(PPh_2py-*P*)] (**1**) (PPh_2py = diphenyl (2-pyridyl)phosphine) has been prepared from $RhCl_3 \cdot 3H_2O$ and PPh_2py and converted to the *trans,cis*-[$RhCl_2$(PPh_2py-*P,N*)$_2$]PF_6 (**2**) in acetone solution by treatment with Ag^+ and PF_6^-. Ruthenium(III) and ruthenium(II) compounds with PPh_2py, *mer,cis*-[$RuCl_3$(PPh_2py-*P,N*)(PPh_2py-*P*)] (**3**) and *mer*-[RuCl(PPh_2py-*P,N*)$_2$(PPh_2py-*P*)]Cl (**5**) have been obtained from DMSO precursor complexes. In a chloroform solution, complex (**5**) isomerizes to *fac*-[RuCl(PPh_2py-*P,N*)$_2$(PPh_2py-*P*)]Cl (*fac*-**5**). All compounds have been characterized by MS, UV–vis, IR, and ^{1}H and ^{31}P{^{1}H} NMR spectroscopy, and the Ru(III) compound has been characterized by EPR spectroscopy as well. The crystal structures of **1**, **2**, **3**, and *fac*-**5** have been determined. In all compounds under investigation, at least one pyridylphosphine acts as a chelate ligand. The ^{31}P chemical shifts for chelating PPh_2py-*P,N* depend on the Ru–P bond lengths.

Introduction

Tertiary phosphines form stable complexes with many transition metals in their various oxidation states. Bidentate ligands containing "soft" phosphorus and "hard" nitrogen donors are extremely useful in both coordination chemistry and homogeneous catalysis. Heterodifunctional ligands exhibit very interesting properties, such as selective binding to metal ions of different types (hard and soft), dynamic behavior via reversible dissociation of the weaker metal−ligand bond, or stereoelectronic control of the coordination sphere of the metal. The P−N ligands with the π-acceptor phosphorus atom can stabilize a low oxidation state of the metal. The σ-donor ability of the nitrogen should help stabilize a higher oxidation state and makes the metal more susceptible to an oxidative addition reaction. Among the most widely studied hemilabile[1] P−N ligands, a prominent position is occupied by the pyridyl phosphines,[2−4] including chiral derivatives.[5] Diphenyl (2-pyridyl)phosphine (PPh_2py) is one of the most useful phosphine ligands applied in coordination chemistry of the transition metals. Four different coordination modes are possible with this compound: P-monodentate,[6,7] N-monodentate,[8] P−N bridge in homo[6c,9−14] and hetero[7,10,15]

* To whom correspondence should be addressed. E-mail: kw@wchuwr.chem.uni.wroc.pl.

(1) (a) Slone, C. S.; Weinberger, D. A.; Mirkin, C. A. *Prog. Inorg. Chem.* **1999**, *48*, 233. (b) Braunstein, P.; Naud, F. *Angew. Chem., Int. Ed.* **2001**, *40*, 680.
(2) Newkome, G. R. *Chem. Rev.* **1993**, *93*, 3, 2067.
(3) Zhang, Z.-Z.; Cheng, H. *Coord. Chem. Rev.* **1996**, *147*, 1.
(4) Espinet, P.; Soulantica, K. *Coord. Chem. Rev.* **1998**, *193*, 499.
(5) Chelucci, G.; Orru, G.; Pinna, G. A. *Tetrahedron* **2003**, *59*, 9471.
(6) (a) Wajda, K.; Pruchnik, F.; Lis, T. *Inorg. Chim. Acta* **1980**, *40*, 207. (b) Schmidbaur, H.; Inoguchi, Y. *Z. Naturforsch. B* **1980**, *35*, 1329. (c) Maisonnat, A.; Farr, J. P.; Balch, A. L. *Inorg. Chim. Acta* **1981**, *53*, L217. (d) Alcock, N. M.; Moore, P.; Lampe, P. A.; Mok, K. F. *J. Chem. Soc., Dalton Trans.* **1982**, 207. (e) Wajda-Hermanowicz, K.; Pruchnik, F. P. *Transition Met. Chem.* **1988**, *13*, 101. (f) Wajda-Hermanowicz, K.; Pruchnik, F. P. *Transition Met. Chem.* **1988**, *13*, 22. (g) Jain, V. K.; Jakkal, V. S.; Bohra, R. *J. Organomet. Chem.* **1990**, *389*, 417. (h) Ang, H. G.; Kwik, W. L.; Lau, P. T. *Polyhedron* **1990**, *9*, 1479. (i) Xie, Y.; James, B. R. *J. Organomet. Chem.* **1991**, *417*, 277. (j) Hirsivaara, L.; Haukka, M.; Pursiainen, *J. Inorg. Chem. Commun.* **2000**, *3*, 508.
(7) Arena, C. G.; Rotondo, E.; Faraone, F. *Organometallics* **1991**, *10*, 3877.
(8) Braunstein, P.; Kelly, D. G.; Tiripicchio, A.; Ugozzoli, F. *Bull. Soc. Chim. Fr.* **1995**, *132*, 1083.
(9) Farr, J. P.; Olmstead, M. M.; Balch, A. L. *J. Am. Chem. Soc.* **1980**, *102*, 2, 6654.
(10) Farr, J. P.; Olmstead, M. M.; Hunt, C. H.; Balch, A. L. *Inorg. Chem.* **1981**, *20*, 1182.
(11) (a) Maekawa, M.; Makata, M.; Kitagawa, S.; Yonezawa, T. *Bull. Chem. Soc. Jpn.* **1991**, *64*, 2286. (b) Cotton, F. A.; Matusz, M. *Inorg. Chim. Acta* **1989**, *157*, 223. (c) Gamasa, M. P.; Gimeno, J.; Lastra, E. *Polyhedron* **1990**, *9*, 2603. (d) Gamasa, M. P.; Gimero, J.; Lastra, E. *J. Organomet. Chem.* **1988**, *346*, 277. (e) Zhang, Z.-Z.; Wang, H.-K.; Xi, Z.; Yao, X.-K.; Wang, R.-J. *J. Organomet. Chem.* **1989**, *376*, 123. (f) Rotondo, E.; Lo Schiavo, S.; Bruno, G.; Arena, C. G.; Gobetto, R.; Faraone, F. *Inorg. Chem.* **1989**, *28*, 2944. (g) Mague, J. T. *Polyhedron* **1990**, *9*, 2635. (h) Cotton, F. A.; Dunbar, K. R.; Matusz, M. *Polyhedron* **1986**, *5*, 903. (i) Schrier, P. W.; Derringer, D. R.; Fanwick, P. E.; Walton, R. A. *Inorg. Chem.* **1990**, *29*, 1290. (j) Roustan, J. L.; Ansari, N.; Ahmed, F. R. *Inorg. Chim.* Acta **1987**, *129*, L11. (k) Xie, Y.; Lee, C.-L.; Yang, Y.; Rettig, S. J.; James, B. R. *Can. J. Chem.* **1992**, *70*, 751.
(12) Bruno, G.; Lo Schiavo, S.; Rotondo, E.; Arena, C. G.; Faraone, F. *Organometallics* **1989**, *8*, 886.

10.1021/ic051442k CCC: $33.50 © 2006 American Chemical Society
Published on Web 03/24/2006

binuclear compounds as well as in oligomers[7,16] and clusters[17] and the P−N chelate mode.[6g,18] Diphenyl (2-pyridyl)-phosphine in its chelating coordination mode forms four-membered rings that are strained and relatively unstable. However, this coordination mode plays a key role in catalysis, e.g., in the carbonylation of alkynes by palladium complexes.[19−21] A detailed knowledge of the ground-state geometry of the metal complexes facilitates a discussion of structure−reactivity relationships. To establish the steric demand of the chelate-coordinated PPh_2py ligand, we prepared and structurally characterized some new rhodium and ruthenium complexes.

Experimental Section

Synthesis. All reactions were performed under an inert atmosphere using standard Schlenk techniques.

The starting complexes *cis*-$RuCl_2(DMSO\text{-}S)_3(DMSO\text{-}O)$[22,23] and *mer*-$RuCl_3(DMSO\text{-}S)_2(DMSO\text{-}O)$[24,25] were prepared according to the literature procedures. $RhCl_3 \cdot 3H_2O$ and PPh_2py (Aldrich) were used as received.

***mer,cis*-[RhCl$_3$(PPh$_2$py-*P,N*) (PPh$_2$py-*P*)] (1).** PPh_2py (0.3 g, 1.14 mmol) in CH_2Cl_2 (15 cm^3) was added with stirring to a warm solution of $RhCl_3 \cdot 3H_2O$ (0.15 g, 0.57 mmol) in anhydrous ethanol (10 cm^3). The mixture was refluxed for 2 h. The resulting orange solution was reduced in volume to about 5 cm^3.The orange complex **1** that deposited was filtered off, washed with diethyl ether, and dried under vacuum (yield: 0.37 g, 88%). Anal. Calcd. for $C_{34}H_{28}Cl_3N_2P_2Rh$ (fw 735.8): C, 55.5; H, 3.8; N, 3.8; Cl, 14.5; P, 8.4. Found: C, 55.1; H, 3.8; N, 3.7; Cl, 14.4; P, 8.0. MS−ESI *m*/*z* (%): 699 (100), $[RhCl_2(PPh_2py)_2]^+$; 664 (58), $[RhCl(PPh_2py)_2]^+$; 627 (10), $[Rh(PPh_2py)_2]^+$. IR (cm^{-1}, KBr): 3058 vw, 1582 vw (ν_{CN}), 1572 w (ν_{CN}), 1482 w, 1449 w, 1434 vs, 1187 vw, 1162 vw, 1020 vw, 998 vw, 766 w, 743 m, 691 vs, 645 vw, 617 vw, 534 s, 521 vs, 505 vs; (Nujol) 495 w, 458 w (δ_{CN}), 443 m (δ_{CN}), 434 m (δ_{CN}), 424 w (δ_{CN}), 417 w, 401 w, 349 vs (ν_{Rh-Cl}), 328 s (ν_{Rh-Cl}), 284 vs (ν_{Rh-Cl}), 258 w, 231 w, 221 s, 210 vw. ^{1}H NMR (CD_2Cl_2, 500 MHz, 298 K): δ 9.17 (t, 1H, H6 py(*P,N*)), 8.26 (d, 1H, H6 py(*P*)), 7.99 (m, 1H, H3 py(*P*)), 7.92−7.85 (m, 4H, H2 Ph(*P*)), 7.72 (m, 1H, H5 py(*P,N*)), 7.54−7.40 (m, 10H, H3 py-(*P,N*), H4 py(*P*), H2 Ph(*P,N*), H4 Ph(*P,N*), H4 Ph(*P*)), 7.33−7.22 (m, 9H, H4 py(*P,N*), H3 Ph(*P,N*), H3 Ph(*P*)), 7.10 (m, 1H, H5 py(*P*)). ^{31}P{^{1}H} NMR (CD_2Cl_2, 500 MHz, 298 K): δ 31.19 (dd, $J_{Rh-P} = 113.2$ Hz, $J_{P-P} = 9.6$ Hz, P(*P*)), −31.97 (dd, $J_{Rh-P} = 100.4$ Hz, $J_{P-P} = 9.6$ Hz, P(*P,N*)). UV−vis (CH_2Cl_2, nm (ϵ, cm^{-1} M^{-1})): 289 (17 240), 366 (1430), 451 (350).

X-ray diffraction quality orange crystals of **1** were isolated from a CH_2Cl_2 solution of the complex that had been layered with EtOH.

***trans*-[RhCl$_2$(PPh$_2$py-*P,N*)$_2$]PF$_6$ (2).** $AgNO_3$ (0.021 g, 0.12 mmol) was added to an acetone (10 cm^3) suspension of **1** (0.09 g, 0.12 mmol), and the mixture was stirred in the dark for 20 min. The AgCl was filtered off through a small Celite plug, and $NaPF_6$ (0.021 g, 0.12 mmol) in acetone (10 cm^3) was added to the resulting yellow solution. After being stirred for ca. 10 min, the solution was concentrated to 5 cm^3 under reduced pressure, and Et_2O (10 cm^3) was added. The yellow solid was collected by suction filtration, washed with Et_2O, and dried under vacuum (yield: 0.0613 g, 60%). Anal. Calcd. for $C_{34}H_{28}Cl_2FN_2P_3Rh$ (fw 845.3): C, 48.3; H, 3.3; N, 3.3. Found: C, 47.9; H, 3.3; N, 3.2. MS−ESI *m*/*z* (%): 699 (100), $[RhCl_2(Ph_2py)_2]^+$; 664 (40), $[RhCl(Ph_2py)_2]^+$. IR (cm^{-1}, KBr): 3443 br/w, 3050 vw, 1584 w (ν_{CN}), 1482 w, 1452 w, 1436 s, 1384 s, 1332 vw, 1281 vw, 1262 vw, 1186 vw, 1162 vw, 1134 vw, 1100 m, 1018 w, 999 vw, 840 vs (ν_{PF}), 767 vw, 741 w, 712 vw, 687 m, 645 vw, 616 vw, 558 s (δ_{PF}), 537 s, 525 m, 513 s; (Nujol) 495 s, 429 m (δ_{CN}), 361 s (ν_{Rh-Cl}), 338 vw, 325 vw, 292 vw, 276 vw, 266 vw, 220 w, 201 m, 160 w.^{1}H NMR ($(CD_3)_2CO$, 300 MHz, 298 K): δ 9.41 (t, 1H, H6 py), 8.58−8.47(m, 3H, H4 Ph + H4 py), 8.18 (m, 1H, H5 py), 7.73−7.65 (m, 4H, H2 Ph), 7.49−7.42 (m, 5H, H3 py + H3 Ph). ^{31}P{^{1}H} NMR ($(CD_3)_2CO$,

(13) Cotton, F. A.; Matusz, M. *Inorg. Chim. Acta* **1988**, *143*, 45.
(14) Rotondo, E.; Bruno, G.; Nicolo, F.; Lo Schiavo, S.; Piraino, P. *Inorg. Chem.* **1991**, *30*, 1195.
(15) (a) Maisonnat, A.; Farr, J. P.; Olmstead, M. M.; Hunt, C. T.; Balch, A. L. *Inorg. Chem.* **1982**, *21*, 3961. (b) Farr, J. P.; Wood, F. E.; Balch, A. L. *Inorg. Chem.* **1983**, *22*, 3387. (c) Farr, J. P.; Olmstead, M. M.; Balch, A. L. *Inorg. Chem.* **1983**, *22*, 1229. (d) Lo Schiavo, S.; Rotondo, E.; Bruno, G.; Faraone, F. *Organometallics* **1991**, *10*, 1613. (e) Zhang, Z.-Z.; Wang, H.-K.; Wang, H.-G.; Wang, R.-J. *J. Organomet. Chem.* **1986**, *314*, 357. (f) Farr, J. P.; Olmstead, M. M.; Rutherford, N. M.; Wood, F. E.; Balch, A. L. *Organometallics* **1983**, *2*, 1758. (g) Zhang, Z.-Z.; Xi, H.-P.; Zhao, W.-J.; Jiang, K.-Y.; Wang, R.-J.; Wu, Y. *J. Organomet. Chem.* **1993**, *454*, 221. (h) Song, H.-B.; Zhang, Z.-Z.; Mak, T. C. W. *New J. Chem.* **2002**, *26*, 113.
(16) (a) Reinhard, G.; Hirle, B.; Schubert, U.; Knorr, M.; Braunstein, P.; DeCian, A.; Fischer, J. *Inorg. Chem.* **1993**, *32*, 1656. (b) Lo Schiavo, S.; Faraone, F.; Franchi, M. L.; Tiripicchio, A. *J. Organomet. Chem.* **1990**, *387*, 357.
(17) (a) Lavigne, G.; Lugan, N.; Bonnet, J.-J. *Organometallics* **1982**, *1*, 1040. (b) Bergounhow, C.; Bonnet, J.-J.; Fompeyrine, P.; Lavigne, G.; Lugan, N.; Mansilla, F. *Organometallics* **1986**, *5*, 60. (c) Wajda-Hermanowicz, K.; Koralewicz, M.; Pruchnik, F. P. *Appl. Organomet. Chem.* **1990**, *4*, 173. (d) Wajda-Hermanowicz, K.; Pruchnik, F. P.; Zuber, M.; Rusek, G.; Gałdecka, E.; Gałdecki, Z. *Inorg. Chim. Acta* **1995**, *232*, 207. (e) Gałdecka, E.; Gałdecki, Z.; Wajda-Hermanowicz, K.; Pruchnik, F. P. *J. Chem. Crystallogr.* **1995**, *25*, 717. (f) Wajda-Hermanowicz, K.; Pruchnik, F. P.; Zuber, M. *J. Organomet. Chem.* **1996**, *508*, 75. (g) Belletti, D.; Graiff, C.; Massera, C.; Predieri, G.; Tiripicchio, A. *Inorg. Chim. Acta* **2003**, *350*, 421. (h) Choi, Y.-Y.; Wong, W.-T. *J. Organomet. Chem.* **1999**, *573*, 189. (i) Hong, F.-E.; Chang, Y.-C.; Chang, R.-E.; Lin, C.-C.; Wang, S.-L.; Liao, F.-L. *J. Organomet. Chem.* **1999**, *588*, 160. (j) Hong, F.-E.; Chen, S.-C.; Tsai, Y.-T.; Chang, Y.-C. *J. Organomet. Chem.* **2002**, *655*, 172. (k) Braunstein, P.; Graiff, C.; Massera, C.; Predieri, G.; Rose, J.; Tripicchio, A. *Inorg. Chem.* **2002**, *41*, 1372.
(18) (a) Jones, N. D.; MacFarlane, K. S.; Smith, M. B.; Schutte, R. P.; Rettig, S. J.; James, B. R. *Inorg. Chem.* **1999**, *38*, 3956. (b) Nishide, K.; Ito, S.; Yoshifuji, M. *J. Organomet. Chem.* **2003**, *682*, 79. (c) Govindaswamy, P.; Mozharivskyj, Y. A.; Kollipara, M. R. *Polyhedron* **2004**, *23*, 3115. (d) Lalrempuia, R.; Carroll, P. J.; Kollipara, M. R. *J. Chem. Sci.* **2004**, *16*, 21. (e) Abram, U.; Alberto, R.; Dilworth, J. R.; Zheng, Y.; Ortner, K. *Polyhedron* **1999**, *18*, 2995. (f) Nicholson, T.; Hirsch-Kuchma, M.; Shellenbarger-Jones, A.; Davison, A.; Jones, A. G. *Inorg. Chim. Acta* **1998**, *267*, 319. (g) Olmstead, M. M.; Maisonnat, A.; Farr, J. P.; Balch, A. L. *Inorg. Chem* **1981**, *20*, 4060. (h) Drommi, D.; Nicolo, F.; Arena, C. G.; Bruno, G.; Faraone, F. *Inorg. Chim. Acta* **1994**, *221*, 109. (i) Li, S.-L.; Mak, T. C. W.; Zhang, Z.-Z. *J. Chem. Soc., Dalton Trans.* **1996**, 3475. (j) Freiberg, E.; Davis, W. M.; Nicholson, T.; Davison, A.; Jones, A. G. *Inorg. Chem.* **2002**, *41*, 5667. (k) Clarke, M. L.; Slawin, A. M. Z.; Wheatley, M. V.; Woollins, J. D. *J. Chem. Soc., Dalton Trans.* **2001**, 3421. (l) Farr, J. P.; Olmstead, M. M.; Wood, F.; Balch, A. L. *J. Am. Chem. Soc.* **1983**, *105*, 792. (m) Baur, J.; Jacobsen, H.; Burger, P.; Artus, G.; Berke, H.; Dahlenburg, L. *Eur. J. Inorg. Chem.* **2000**, 1411. (n) Moldes, I.; De la Encarnacion, E.; Ros, J.; Alvarez-Larena, A.; Piniella, J. F. *J. Organomet. Chem.* **1998**, *566*, 165. (o) Suzuku, T.; Kuchiyama, T.; Kishi, S.; Kaizaki, S.; Kato, M. *Bull. Chem. Soc. Jpn.* **2002**, *75*, 2433.
(19) Drent, E.; Arnoldy, P.; Budzelaar, P. H. M. *J. Organomet. Chem.* **1993**, *455*, 247.
(20) Consorti, C. S.; Ebeling, G.; Dupont, J. *Tetrahedron Lett.* **2002**, *43*, 753.
(21) Drent, E.; Arnoldy, P.; Budzelaar, P. H. M. *J Organomet. Chem.* **1994**, *475*, 57.
(22) Evans, I. P.; Spencer, A.; Wilkinson, G. *J. Chem. Soc., Dalton Trans.* **1973**, 204.
(23) Alessio, E.; Mestroni, G.; Nardin, G.; Attia, W. M.; Calligaris, M.; Sava, G.; Zorzet, S. *Inorg. Chem.* **1988**, *27*, 4099.
(24) McMillan, R. S.; Mercer, A.; James, B. R.; Trotter, J. *J. Chem. Soc., Dalton Trans.* **1975**, 1006.
(25) Alessio, E.; Balducci, G.; Calligaris, M.; Costa, G.; Attia, W. M.; Mestroni, G. *Inorg. Chem.* **1991**, *30*, 609.

300 MHz, 298 K): δ −15.1 (d, J_{Rh-P} = 93.9 Hz), −144.27 (sep, J_{P-F} = 713 Hz). UV−vis (acetone, nm (ϵ, cm^{-1} M^{-1})): 295 (60 200), 328 (1880), 424 (280).

Yellow crystals of **2-$(CH_3)_2CO$** were grown by freezing an acetone solution of **2** into which Et_2O had been added.

***mer,cis*-[$RuCl_3$(PPh_2py-*P*,*N*)(Ph_2py-*P*)] (3).** *mer*-[$RuCl_3$(DMSO-*S*)$_2$(DMSO-*O*)] (0.0442 g, 0.1 mmol) was dissolved in CH_2Cl_2 (5 cm^3). Ph_2py (0.0526 g, 0.2 mmol) in the same solvent (5 cm^3) was added, and the resulting mixture was stirred at room temperature for 3 h. The resulting red-orange solution was reduced in volume to about 5 cm^3 and Et_2O (25 cm^3) was added, giving an orange solid. This precipitate was filtered off, washed with diethyl ether, and dried under vacuum (yield: 0.0624 g, 85%). Anal. Calcd. for $C_{34}H_{28}Cl_3N_2P_2Ru$ (fw 734.0): C, 55.6; H, 3.9; N, 3.8; Cl, 14.5; P, 8.4. Found: C, 55.2; H, 3.8; N, 3.7; Cl, 14.3; P, 8.0. MS−ESI *m*/*z* (%): 697 (50), $[RuCl_2(Ph_2py)_2]^+$; 662 (100), $[RuCl(Ph_2py)_2]^+$; 626 (10), $[Ru(Ph_2py)_2]^+$. IR (cm^{-1}, KBr): 3440 m, 3057 vw, 1582 vw (ν_{CN}), 1571 w (ν_{CN}), 1481 m, 1448 w, 1434 vs, 1330 vw, 1309 vw, 1270 vw, 1186 vw, 1162 vw, 1131 vw, 1092 m, 1017 w, 998 vw, 986 vw, 765 m, 743 m, 727 w, 691 vs, 642 vw, 617 vw, 568 vw, 531 vs, 516 vs; (Nujol) 497 vs, 455 m (δ_{CN}), 443 m (δ_{CN}), 431 m (δ_{CN}), 424 m (δ_{CN}), 416 w, 400 w, 339 vs (ν_{Ru-Cl}), 323 s (ν_{Ru-Cl}), 282 vs (ν_{Ru-Cl}), 255 w, 230 w, 214 w. UV−vis ($CHCl_3$, nm (ϵ, cm^{-1} M^{-1})): 248 (12 850), 364 (2510), 447 (1040), 504 (690).

Orange single crystals of **3** appropriate for X-ray measurements were grown from chloroform/ether via the slow vapor diffusion technique.

[NBu_4][*mer*-$RuCl_3$(DMSO-*S*)$_3$] (4). *Cis*-$RuCl_2$(DMSO-*S*)$_3$-(DMSO-*O*) (0.024 g, 0.05 mmol) was dissolved in 10 cm^{-3} of a 1:1 mixture of CH_2Cl_2 and CH_3OH, and 0.015 g of [NBu_4]Cl·H_2O (0.05 mmol) was then added. The yellow solution was refluxed for 15 min and vacuum-evaporated to 2 cm^3. Et_2O (10 cm^3) was then added. The yellow solid was collected by filtration, washed several times with Et_2O, and dried in a vacuum (yield: 0.024 g, 68%). Anal. Calcd. for $C_{22}H_{54}Cl_3NRuS_3O_3$ (fw 684.3): C, 38.6; H, 8.0; N, 2.1; S, 14.1. Found: C, 38.4; H, 8.0; N, 2.1; S, 14.0. MS−ESI *m*/*z* (%): 441 (75), $[RuCl_3(DMSO)_3]^-$; 363 (100), $[RuCl_3$-$(DMSO)_2]^-$. IR (cm^{-1}, KBr): 3405 br/vs, 2960 vs (cation), 2874 vs (cation), 1634 m, 1487 vs (cation), 1382 s (cation), 1307 w, 1287 vw, 1151 w, 1105 s (ν_{S-O}), 1081 s (ν_{S-O}), 1028 s, 973 w, 925 vw, 882 m (cation), 800 vw, 739 w, 709 vw, 676 w; (Nujol) 425 s (ν_{Ru-S}), 384 m (δ_{CSO}), 345 m (ν_{Ru-Cl}), 334 sh/m (ν_{Ru-Cl}), 297 w (ν_{Ru-Cl}), 266 w, 241 w.

***mer*-[Ru Cl(PPh_2py-*P*,*N*)$_2$(PPh_2py-*P*)]Cl (5).** A solution of PPh_2py in acetone (10 cm^3) was added dropwise (0.0237 g, 0.09 mmol) to an acetone (5 cm^3) solution of **4** (0.0205 g, 0.03 mmol). The mixture was stirred at room temperature for 3 h. The solution was concentrated and Et_2O (20 cm^3) was added, giving an orange solid. This was filtered off, washed with diethyl ether, and dried under vacuum (yield: 0.0066 g, 23%). Anal. Calcd. for $C_{51}H_{42}$-$Cl_2N_3P_3Ru$ (fw 961.8): C, 63.7; H, 4.4; N, 4.4; Cl, 7.4. Found: C, 63.5; H, 4.4; N, 4.4; Cl, 7.2. MS−ESI *m*/*z* (%): 926 (8), $[RuCl$-$(Ph_2py)_3]^+$; 663 (100), $[RuCl(Ph_2py)_2]^+$. IR (cm^{-1}, KBr): 3434 br/s, 3049 w, 1583 vw (ν_{CN}), 1571 w (ν_{CN}), 1482 w, 1444 w, 1435 vs, 1309 vw, 1262 w, 1186 w, 1158 w, 1119 m, 1096 s, 1022 w, 998 vw, 802 vw, 772 w, 766 w, 745 m, 724 w, 697 s, 618 vw, 522 s, 514 s; (Nujol) 493 s, 466 m (δ_{CN}), 445 m (δ_{CN}), 433 m (δ_{CN}), 424 m (δ_{CN}), 279 m (ν_{Ru-Cl}), 264 vw, 254 vw, 229 vw, 203 vw. ^{1}H NMR ($(CD_3)_2CO$, 300 MHz, 298 K): δ 9.07 (t, H6 py(*P*,*N*)), 8.4−6.45 (m, H py + H Ph phosphine ligands). $^{31}P\{^1H\}$ NMR ($(CD_3)_2CO$, 300 MHz, 298 K): δ 53.05 (t, J_{P-P} = 30.5 Hz, $P_{terminal}$), −2.80 (d, $P_{chelate}$).

***fac*-[RuCl(PPh_2py-*P*,*N*)$_2$(PPh_2py-*P*)]Cl (*fac*-5).**[18h] X-ray diffraction quality orange crystals of *fac*-**5**·**2$CHCl_3$** were isolated from a $CHCl_3$ solution of complex **5** that had been layered with Et_2O.

Physical Measurements. IR spectra were recorded on a Bruker IFS113v; UV−vis spectra were recorded on Bruker DU 7500 and Cary 5 spectrometers. Electrospray mass spectra were recorded on a Finnigan MAT TSQ 700 triple stage quadrupole mass spectrometer equipped with an electrospray ion source. EPR spectra were measured on a Bruker ESP 300E spectrometer equipped with a variable-temperature accessory and a liquid N_2 Dewar insert. The ^{1}H and $^{31}P\{^1H\}$ NMR spectra were recorded on Bruker AMX 300 and Avance 500 spectrometers. The chemical shifts in the ^{1}H NMR spectra were referenced to the residual proton impurities in the deuterated solvents and $^{31}P\{^1H\}$ NMR spectra to external 85% H_3PO_4. Conductivity measurement was made at 25 °C on freshly made 0.5 mM solution of a complex in acetone, using an electrochemical meter universal instrument (Technical University Wrocław, Poland). The magnetic susceptibility was measured using a Quantum Design SQUID magnetometer (type MPMS-5). The magnetic moment values were calculated after considering the appropriate diamagnetic corrections.

X-ray Structural Determination. The studied crystals were mounted onto a glass fiber and then flash-frozen to 100 K (Oxford Cryosystem cooler). Preliminary examination and intensity data collection were carried out on a Kuma KM4CCD κ-axis diffractometer with graphite-monochromated Mo Kα radiation (λ = 0.71073 Å). Crystals were positioned at 65 mm from the CCD camera. A total of 612 frames were measured at 0.75° intervals with a counting time of 15−20 s. Accurate cell parameters were determined and refined by least-squares fit of 3900−7000 of the strongest reflections. The data were corrected for Lorentz and polarization effects, and the analytical absorption corrections were also applied. Data reduction and analysis were carried out with the Oxford Diffraction (Poland) programs. Structures were solved by the heavy atom method (program SHELXS97[26]) and refined by the full-matrix least-squares method on all F^2 data using the SHELXL97[27] programs. Non-hydrogen atoms were refined with anisotropic displacement parameters; hydrogen atoms were included from geometry of molecules and $\Delta\rho$ maps. They were treated as riding groups during the refinement process. The absolute structures of chiral crystals were determined by Flack's method.[28] Crystal data are given in Table 1, together with refinement details.

Results and Discussion

Rhodium Complexes. Diphenyl (2-pyridyl)phosphine is a potentially P−N chelating ligand, but the rhodium(I) metal center seems to favor a bidentate bridging coordination.[9,12,29] Up to now, the P−N chelation to rhodium(I) was postulated only by Faraone for cationic complex [Rh(COD)(PPh_2py)]X (X = ClO_4, PF_6). The P−N chelate coordination was supported only by chemical analysis, IR spectra, and conductivity measurements; NMR spectra and X-ray structure were not investigated.[7] It is well-known that rhodium(II) complexes are binuclear with a PPh_2py molecule coordinated as a bidentate bridging ligand.[13,14] The compound [Cp*RhCl-(PPh_2py-*P*,*N*)]ClO_4[18k] is the only known example of P−N

(26) Sheldrick, G. M. *SHELXS97*: *Program for Solution of Crystal Structures*; University of Göttingen: Göttingen, Germany, 1997.
(27) Sheldrick, G. M *SHELXL97*: *Program for Crystal Structure Refinement*; University of Göttingen: Göttingen, Germany, 1997.
(28) Flack, H. D. *Acta Crystallogr., Sect. A* **1983**, *39*, 876.
(29) Mague, J. T. *Orgamometallics* **1986**, *5*, 918.

Table 1. Crystal Data and Structure Refinement for $RhCl_3(PPh_2py\text{-}P,N)(PPh_2py\text{-}P)$ (**1**), $[RhCl_2(PPh_2py\text{-}P,N)_2]PF_6$ (**2**), $RuCl_3(PPh_2py\text{-}P,N)(PPh_2py\text{-}P)$ (**3**), and $[RuCl(PPh_2py\text{-}P,N)_2(PPh_2py\text{-}P)]Cl$ (*fac*-**5**)

	1	**2**	**3**	*fac*-**5**
empirical formula	$C_{34}H_{28}N_2Cl_3P_2Rh$	$C_{37}H_{34}F_6N_2OCl_2P_3Rh$	$C_{34}H_{28}N_2Cl_3P_2Ru$	$C_{53}H_{44}N_3Cl_8P_3Ru$
fw	735.78	903.38	733.94	1200.49
T (K)	100(2)	100(2)	100(2)	100(2)
λ (Å)	0.71073	0.71073	0.71073	0.71073
cryst syst	orthorhombic	orthorhombic	monoclinic	triclinic
space group	$P2_12_12_1$	$P2_12_12$	$P2_1/n$	$P\bar{1}$
a (Å)	11.0841(8)	13.2352(9)	9.046(2)	11.781(2)
b (Å)	14.9184(12	11.0135(9)	21.331(4)	15.449(3)
c (Å)	18.5128(14	13.1525(12)	16.040(3)	17.961(4)
α (deg)	90	90	90	67.72(3)
β (deg)	90	90	90.21(3)	85.64(3)
γ (deg)	90	90	90	76.35(3)
V (Å^3)	3061.2(4)	1917.2(3)	3095.1(11)	2939.2(10)
Z	4	2	4	2
D_c (mg m^{-3})	1.596	1.565	1.575	1.356
μ (mm^{-1})	0.953	0.772	0.897	0.748
F(000)	1488	912	1484	1216
cryst size (mm^3)	0.16 × 0.12 × 0.09	0.22 × 0.18 × 0.15	0.12 × 0.08 × 0.06	0.15 × 0.15 × 0.10
θ range for data collection (deg)	3.29−27.00	3.45−27.00	3.22−27.00	2.88−27.00
ranges of h,k,l	$-14 < h < 8$, $-19 < k < 19$, $-23 < l < 23$	$-16 < h < 16$, $-12 < k < 14$, $-13 < l < 16$	$-11 < h < 8$, $-27 < k < 27$, $-20 < l < 20$	$-15 < h < 15$, $-19 < k < 19$, $-22 < l < 16$
no. of reflns collected	20 492	12 782	30 232	38 268
no. of independent reflns (R_{int})	6566 (0.0711)	4144 (0.0350)	6755 (0.1240)	12798 (0.0980)
data/params	6566/380	4144/239	6755/379	12798/613
abs coeff min/max	0.863/0.919	0.848/0.893	0.900/0.948	0.896/0.929
GOF (F^2)	0.920	1.082	1.201	1.123
final R_1/wR_2 indices ($I > 2\sigma_I$)	0.0475/0.0484	0.0342/0.0749	0.0762/0.1693	0.0883/0.1810
extinction coeff	0.00050(9)	0.0009(4)		
largest diff peak/hole (e Å^{-3})	0.408/−0.454	0.801/−0.914	1.548/−0.936	1.304/−1.387
Flack's param	−0.06(3)	−0.01(3)		

chelate coordination to rhodium. For this reason, the rhodium(III) metal center should be a good candidate for preparation of such complexes with a PPh_2py molecule.

The reaction of two moles of PPh_2py with one mole of $RhCl_3{\cdot}3H_2O$ in ethanolic solution at room temperature gave an air-stable, orange solid of formula $[RhCl_3(PPh_2py)_2]$. The ESI(+) MS shows no parent ion but does show fragments $[RhCl_2(Ph_2py)_2]^+$, $[RhCl(Ph_2py)_2]^+$, and $[Rh(Ph_2py)_2]^+$ (with the correct isotopic distributions) that correspond to the peaks at m/z 699, 664, and 627, respectively. Two different pyridylphosphine moieties are detected by NMR. In the ^{1}H NMR spectrum, the H6 atoms of pyridyl appear as two signals, a doublet at 8.26 ppm and a triplet at 9.17 ppm. The downfield-shifted resonance is assigned to the chelating ligand coupling also with Rh ($^3J_{H-H} = {}^3J_{Rh-H} = 4.3$ Hz). Two doublets of doublets are observed in the $^{31}P\{^1H\}$ NMR spectrum. The low-field signal at δ 31.19 ppm is assigned to the terminal pyridylphosphine ligand and the second one at δ −31.97 ppm to the chelating phosphine ligand. An upfield shift in the ^{31}P NMR spectrum (relative to the monodentate coordination) is known to be diagnostic of a four-membered chelating ring.[30,31] This indicates that the one PPh_2py molecule is coordinated as a terminal ligand and the second one as a chelating ligand through P and N atoms. For this type of coordination, as seen in Figure 1, there are three possible geometrical isomers for an octahedral compound of general formula $[RhCl_3(PPh_2py\text{-}P,N)(PPh_2py\text{-}P)]$. The ^{1}H and ^{31}P NMR spectra showed that only one isomer was formed. The small $^2J_{PP}$ value (9.6 Hz) indicates that phosphine ligands occupy cis coordination sites. The trans $^2J_{pp}$ is usually large, a few hundred Hz, whereas the cis coupling constant is small.[32] Of the two ^{31}P NMR resonances, the one at lower frequency with a smaller $^1J_{Rh-P}$ is assigned to the phosphorus trans to the chlorine atom. The other resonance at higher frequency with $^1J_{Rh-P} = 113.2$ Hz is assigned to the phosphine ligand trans to the nitrogen atom. The $^1J_{Rh-P}$ value (100.4 Hz) for the phosphine trans to the chlorine is smaller than the values reported for rhodium(III) complexes of the type *mer*-$[RhCl_3(PR_3)_3]$, in which the phosphine ligand is trans to chlorine.[32] The lower value of $^1J_{Rh-P}$ indicates a longer Rh−P distance, probably because of the strain in the four-membered chelating ring. Coordination of the N atom of PPh_2py to a metal ion is expected to shift the IR bands of the pyridine ring to higher frequencies by 10−30 cm^{-1}.[33] The band located at 1582 cm^{-1} is assigned to the ν(C═N) stretching vibration. The energy of this band is lower in comparison with that of the free PPh_2py ligand and indicates the presence of N-coordinated pyridyl. The far-IR spectrum shows three ν(Rh−Cl) bands in the region 350−280 cm^{-1} (349, 328, and 284 cm^{-1}), which are expected for the mer geometry.[34] All above results allow us to concluded that complex **1** is the mononuclear mer,cis isomer (Figure 1) with monodentate and bidentate pyridylphosphine ligands.

(30) Garrou, P. E. *Chem. Rev.* **1981**, *81*, 229.
(31) Hietkamp, S.; Stufkens, D. J.; Vrieze, K. *J. Organomet. Chem.* **1979**, *169*, 107.
(32) Pregosin, P. S.; Kunz, R. W. *^{31}P and ^{13}C NMR of Transition Metal Phosphine Complexes*; Springer-Verlag: Berlin, 1979.
(33) Dahlhoff, W. V.; Dick, T. R.; Ford, G. H.; Neoson, S. M. *J. Inorg. Nucl. Chem.* **1971**, *33*, 1799.
(34) Mann, B. E.; Masters, C.; Shaw, B. L. *J. Chem. Soc., Dalton Trans* **1973**, 1489.

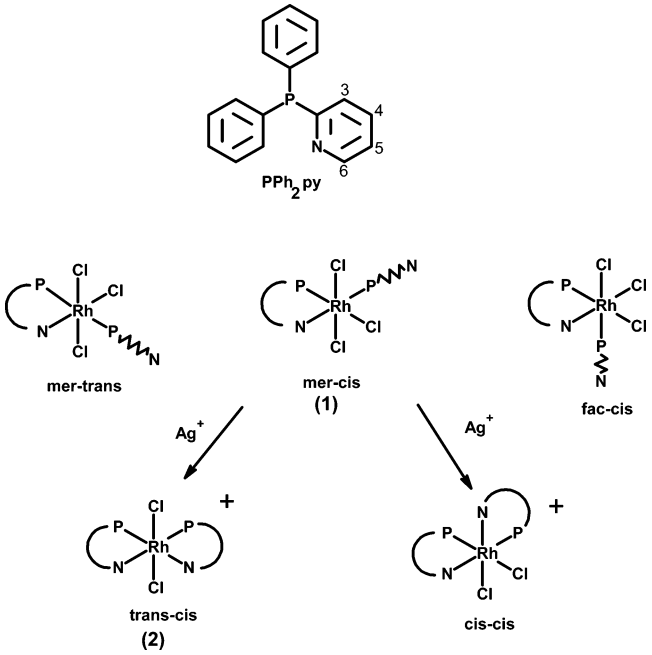

Figure 1. Possible isomers for compounds of general formula $[RhCl_3(PPh_2py\text{-}P,N)(PPh_2py\text{-}P)]$ and $[RhCl_2(PPh_2py\text{-}P,N)_2\}^+$.

The electronic spectra of Rh(III) octahedral complexes are expected to contain two d−d transitions from the $^1A_{1g}$ ground state to $^1T_{1g}$ and $^1T_{2g}$ (for O_h symmetry), but the higher-energy transition to $^1T_{2g}$ is rarely detectable because it is hidden beneath the intense CT transitions.[35] The absorption spectrum of complex **1** in dichloromethane solution exhibits three bands at 289 nm (ϵ = 17 240), 366 nm (ϵ = 1430), and 451 nm (ϵ = 350). The band observed at 289 nm is considered to be due to intraligand $n\pi^*$ transition.[36] The low-energy band at 451 nm should be assigned to the spin-allowed $^1T_{1g} \leftarrow {}^1A_{1g}$ transition. This transition in complex $[RhCl_3(tpy)]$ (tpy = 2,2′:6′,2″-terpyridine) is observed at similar energy (421 nm).[37] The band at 366 nm is assigned to the MLCT transition.

Crystallization of complex **1** from CH_2Cl_2 after layering with EtOH yielded crystals suitable for a crystal-structure determination. The crystal structure of **1** (Figure 2) shows the rhodium center to be approximately octahedral, with three chlorine ligands occupying meridional positions. The two PPh_2py ligands are cis to one another and adopt two different bonding modes, chelating and monodentate. Selected bond lengths and angles are listed in Table 2. The mer,cis isomer (Figure 1) of complex **1** can exist only as one achiral stereoisomer. The single-crystal X-ray analyses revealed that compound **1** crystallizes in isomorphous space group $P2_12_12_1$, which is indicative of the spontaneous resolution of the enantiomeric pair. The chirality occurs at the metal center, but **1** is not chiral in solution because of the fluxionality of the arms of PPh_2py. One can note that under crystallization conditions, two enantiomorphic crystals were formed. The

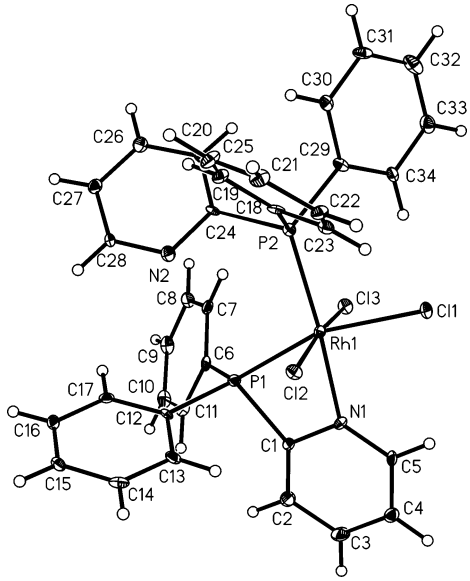

Figure 2. Molecular structure of $[RhCl_3(PPh_2py\text{-}P)(PPh_2py\text{-}P,N)]$ (**1**) with crystallographic numbering.

central Rh(III) has a distorted octahedral coordination due to the presence of a four-membered chelating ligand with the bite angle substantially reduced from the regular cis angle of 90° to N(1)−Rh−P(1) = 69.21(10)°, which is similar to that observed for the rhodium(III) compound containing orthometalated triphenylphosphine $[Rh(C_6H_4PPh_2\text{-}C,P)_3]$ (68−69°).[38] The Rh−Cl bond lengths are 2.3534(11), 2.3605(11), and 2.3852(10) Å. The Rh−Cl bond trans to the phosphine ligand is longer than other bonds. The Rh−P bond trans to Cl is longer (2.3184(12) Å) than that trans to the N atom of the pyridyl ring (2.3045(12) Å). Similar trends were also observed for similar compounds of Tc(III) and Ru(III) (Table 2).

Coordination of the second pyridine nitrogen ligand to rhodium in **1** has been achieved by removing the chloride with $AgNO_3$ in an acetone solution (Figure 1). In the presence of NH_4PF_6, cationic complex $[RhCl_2(PPh_2py)_2]PF_6$ **2** was isolated as a yellow solid. Conductivity measurements in an acetone solution (Λ = 119 Ω^{-1} cm^2 mol^{-1} in 1 × 10^{-4} M solution) indicated that **2** is a 1:1 electrolyte.[39] The electrospray mass spectra of **2** revealed peaks with the correct isotopic distributions at m/z = 699 and 664, corresponding to the $[RhCl_2(PPh_2py)_2]^+$ and $[RhCl(PPh_2py)_2]^+$ ions, respectively. The IR spectrum of **2** shows the characteristic strong absorption of the PF_6^- anion at 840 and 558 cm^{-1}. The ν(C═N) band (1584 cm^{-1}) can be assigned to the coordinated pyridyl groups. A single Rh−Cl stretching vibration at 361 cm^{-1} indicated that two chloride ligands are in the trans positions. The ^{1}H and $^{31}P\{^1H\}$ NMR spectra show that both phosphine molecules are equivalent chelating ligands. This is confirmed by the presence of a triplet at 9.41 ppm, assigned to the H6 protons of pyridyl rings ($^3J_{H5-H6} = {}^3J_{Rh-H6}$ = 3 Hz) in the ^{1}H NMR spectrum, and a doublet at δ = −15.1 ($^1J_{Rh-P}$ = 93.9 Hz) in $^{31}P\{^1H\}$ NMR. A septet

(35) Lever, A. B. P. *Inorganic Electronic Spectroscopy*, 2nd ed.; Elsevier: Amsterdam, 1984.
(36) Vogler, A.; Kunkely, H. *Coord. Chem. Rev.* **2002**, *230*, 243.
(37) Pruchnik, F. P.; Jakimowicz, P.; Ciunik, Z.; Zakrzewska-Czerwiñska, J.; Opolski, A.; Wietrzyk, J.; Wojdat, E. *Inorg. Chim. Acta* **2002**, *334*, 59.
(38) Bennett, M. A.; Bhargava, S. K.; Ke, M.; Willis, A. C. *J. Chem. Soc., Dalton Trans.* **2000**, 3537.
(39) Geary, W. J. *Coord. Chem. Rev.* **1971**, *7*, 81.

Table 2. Selected Bond Lengths (Å) and Angles (deg) for $RhCl_3(PPh_2py\text{-}P)(PPh_2py\text{-}P,N)$ (**1**), $RuCl_3(PPh_2py\text{-}P)(PPh_2py\text{-}P,N)$ (**3**), and $TcCl_3(PPh_2py\text{-}P)(PPh_2py\text{-}P,N)$[18j]

$TcCl_3(PPh_2py)_2$ d^4		$RuCl_3(PPh_2py)_2$ d^5		$RhCl_3(PPh_2py)_2$ d^6	
Tc−N(1)	2.150(4)	Ru−N(1)	2.172(5)	Rh−N(1)	2.085(3)
Tc−P(1)	2.4554(15)	Ru−P(1)	2.4152(17)	Rh−P(1)	2.3184(12)
Tc−P(2)	2.4325(15)	Ru−P(2)	2.3192(18)	Rh−P(2)	2.3045(12)
Tc−Cl(1)	2.4174(140	Ru−Cl(1)	2.3728(15)	Rh−Cl(1)	2.3852(10)
Tc−Cl(2)	2.3403(15)	Ru−Cl(2)	2.3330(14)	Rh−Cl(2)	2.3534(11)
Tc−Cl(3)	2.3338(14)	Ru−Cl(3)	2.3386(15)	Rh−Cl(3)	2.3605(11)
N(1)−Tc−P(2)	173.599(13)	N(1)−Ru−P(2)	172.64(13)	N(1)−Rh−P(2)	175.717(10)
N(1)−Tc−P(1)	66.36(12)	N(1)−Ru−P(1)	66.62(13)	N(1)−Rh−P(1)	69.21(10)
P(2)−Tc−P(1)	107.24(5)	P(2)−Ru−P(1)	107.51(5)	P(2)−Rh−P(1)	106.56(4)
N(1)−Tc−Cl(2)	87.21(12)	N(1)−Ru−Cl(2)	82.68(12)	N(1)−Rh−Cl(2)	86.57(10)
P(2)−Tc−Cl(2)	92.13(6)	P(2)−Ru−Cl(2)	92.84(5)	P(2)−Rh−Cl(2)	93.72(4)
P(1)−Tc−Cl(2)	86.16(5)	P(1)−Ru−Cl(2)	87.78(5)	P(1)−Rh−Cl(2)	90.24(4)
N(1)−Tc−Cl(3)	87.57(12)	N(1)−Ru−Cl(3)	92.43(12)	N(1)−Rh−Cl(3)	86.83(9)
P(2)−Tc−Cl(3)	92.60(5)	P(2)−Ru−Cl(3)	91.37(6)	P(2)−Rh−Cl(3)	92.84(4)
P(1)−Tc−Cl(3)	88.00(5)	P(1)−Ru−Cl(3)	84.57(5)	P(1)−Rh−Cl(3)	87.17(4)
Cl(2)−Tc−Cl(3)	173.36(5)	Cl(2)−Ru−Cl(3)	172.10(5)	Cl(2)−Rh−Cl(3)	173.40(4)

typical of the PF_6^- anion was observed at −144.27 ppm. As expected, the PPh_2py:PF_6^- signal ratio is 2:1. The absorption spectrum of complex **2** in acetone solution is similar to that of **1** and exhibits three bands at 295 (60 200), 328 (1880), and 424 (280) nm, which are assigned to intraligand $n\pi^*$, MLCT, and the spin-allowed $^1T_{1g} \leftarrow {}^1A_{1g}$ transitions, respectively.

Compound **2** crystallized in the chiral space group $P2_12_12$ with two molecules in the unit cell. The crystal structure consists of $[RhCl_2(PPh_2py)_2]^+$ cations, PF_6^- anions, and solvate $(CH_3)_2CO$ molecules, held together by electronic and van der Waals interactions. The rhodium, PF_6^- anions, and acetone molecules are situated on a 2-fold axis. Rh(III) in the cation is situated in a distorted octahedral coordination environment, with two chloride ligands in the trans positions and two chelated P−N ligands in cis positions (Figure 3). The five atoms Rh, P1, P1*, N1, and N1* and two pyridyl rings are coplanar. The selected bond distances and angles for **2** are listed in Table 3. The crystals of **2** are an example of the chiral crystallization of achiral compounds, which is common for inorganic, organic, and organometallic compounds.[40] The Rh−P and Rh−Cl distances are shorter than those observed in **1** (Table 2) or in Rh(III) *trans*-$[RhCl_2(P-P)_2]^+$ type complexes[41] for about 0.05 and 0.02 Å, respectively. However, the Rh−N bond lengths found in **2** are longer (by at least 0.06 Å) than that in **1**. The N−Rh−N and P−Rh−P angles are in the range 110.73−111.57°, whereas P−Rh−N angles are smaller (68.86°) because of strain in the four-membered rings.

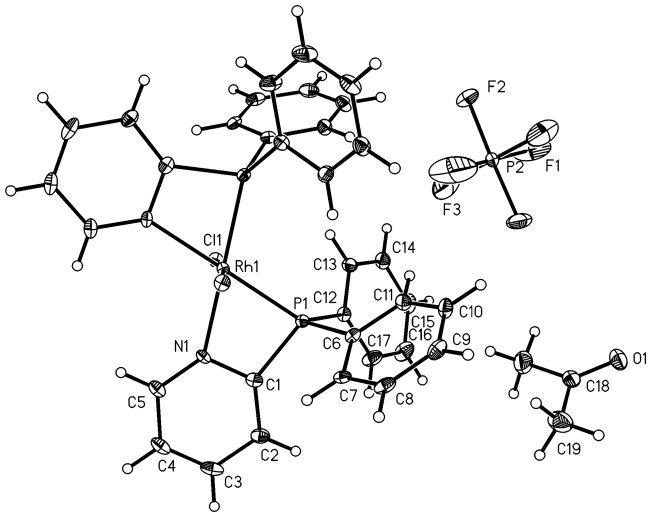

Figure 3. Molecular structure of $[RhCl_2(PPh_2py\text{-}P,N)_2]PF_6$ (**2**) with crystallographic numbering.

Table 3. Selected Bond Lengths (Å) and Angles (deg) for *trans*-$[RhCl_2(PPh_2py\text{-}P,N)_2]PF_6$ (**2**)

Rh(1)−N(1)	2.149(3)		
Rh(1)−P(1)	2.2731(10)		
Rh(1)−Cl(1)	2.3361(7)		
N(1)−Rh(1)−N(1)#1	110.73(15)	P(1)−Rh(1)−Cl(1)#1	92.41(3)
N(1)−Rh(1)−P(1)#1	178.79(8)	N(1)−Rh(1)−Cl(1)	88.71(7)
N(1)−Rh(1)−P(1)	68.86(8)	P(1)#1−Rh(1)−Cl(1)	92.41(3)
P(1)#1−Rh(1)−P(1)	111.57(5)	P(1)−Rh(1)−Cl(1)	90.70(3)
N(1)−Rh(1)−Cl(1)#1	88.15(7)	Cl(1)#1−Rh(1)−Cl(1)	174.48(4)

Ruthenium Complexes. The DMSO ruthenium compounds are useful precursors for the syntheses of ruthenium complexes with P−N chelating ligands. Replacement of all the DMSO ligands was obtained upon treatment of the ruthenium complexes with P or N donor ligands under mild conditions.[22]

A paramagnetic complex of formula $[RuCl_3(PPh_2py)_2]$ (**3**) was obtained from *mer*-$[RuCl_3(DMSO\text{-}S)_2(DMSO\text{-}O)]$ and PPh_2py in a CH_2Cl_2 solution at room temperature. The ESI(+) MS spectrum of **3** is similar to that of *mer,cis*-$[RhCl_3(PPh_2py\text{-}P,N)(PPh_2py\text{-}P)]$ (**1**). The ions $[RuCl_2(PPh_2py)_2]^+$ (m/z = 697), $[RuCl(PPh_2py)_2]^+$ (m/z = 662), and $[Ru(PPh_2py)_2]^+$ (m/z = 626) were observed. As expected, the IR spectrum of **3** is also very similar to that observed for **1** and contains weak bands at 1582 and 1571 cm^{-1} assigned to the ν(C=N) vibration of N-coordinated and noncoordinated pyridyl rings, respectively. Three ν(Ru−Cl) bands at 339, 323, and 282 cm^{-1} reveal a mer arrangement of chlorides.[42] Solid-state magnetic moment measurement at 290 K suggests that complex **3** is paramagnetic with a magnetic moment (μ = 1.92 μ_B) corresponding to one unpaired electron.[42] A powdered sample of **3** at 77 K exhibits

(40) Matsuura, T.; Koshima, H. *J. Photochem. Photobiol., C* **2005**, *6*, 7−24.
(41) Hill, A. M.; Levason, W.; Preece, S. R.; Webster, M. *Polyhedron* **1997**, *16*, 1307.
(42) Ruiz-Ramirez, L.; Stephenson, T. A.; Switkes, E. S. *J Chem. Soc., Dalton Trans.* **1973**, 1770.

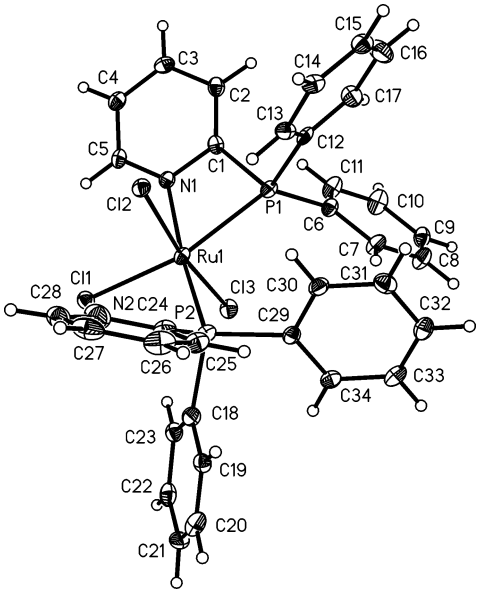

Figure 4. Molecular structure of [$RuCl_3$(PPh_2py-*P*)(PPh_2py-*P*,*N*)] (**3**) with crystallographic numbering.

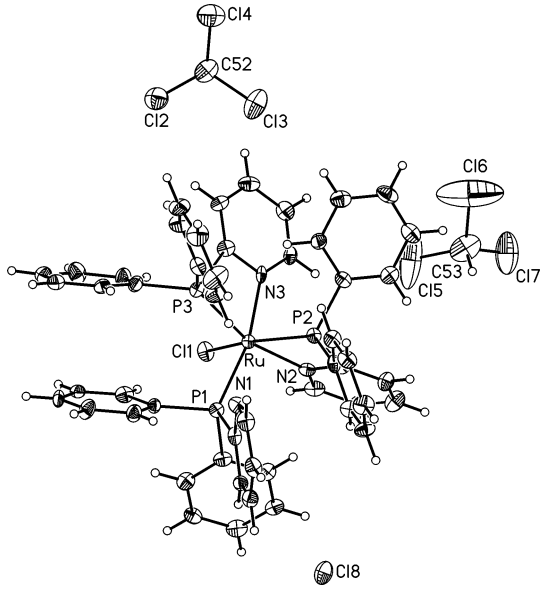

Figure 5. Molecular structure of [RuCl((PPh_2py-*P*)(PPh_2py-*P*,*N*)$_2$]Cl (*fac*-**5**) with crystallographic numbering.

an EPR spectrum with three *g* values ($g_1 = 2.69$, $g_2 = 2.15$, and $g_3 = 1.72$), typical of rhombic low-spin d^5 Ru(III) complexes.[43] The complex absorbs strongly in the 248−504 nm region {248 ($\epsilon = 12850$), 364 ($\epsilon = 2510$), 447 ($\epsilon = 1040$), 504 ($\epsilon = 690$) nm, presumably due to the intraligand and charge-transfer transitions. The spectrum is similar to that observed for the d^5 ruthenium(III) compounds containing PPh_3, N-donors (pyridine, bipyridine, or phenanthroline), and Cl ligands.[42]

The molecular structure of **3** (Figure 4) was determined by X-ray crystallography. As expected, the compound is a monomeric six-coordinate complex with mer chloride ligands and two cis PPh_2py molecules in two different bonding modes, monodentate and chelating. Selected bond lengths and angles are listed in Table 2. Table 2 also shows that the molecular structures of Tc, Ru, and Rh compounds are nearly identical. The P−M−N bite angles of a four-membered metallacycle for Tc(d^4), Ru(d^5), and Rh(d^6) species are equal to 66.36(12), 66.62(13), and 69.21(10)°, respectively. The M−P distances, for both chelating and nonchelating phosphine, diminish with an increase in the number of d electrons from d^4 to d^6 (2.4554(15), 2.4152(17), and 2.3184(12) Å for $M-P_{chelate}$ and 2.4325(15), 2.3192(18), and 2.3045(12) Å for $M-P_{terminal}$). On the other hand, the Ru−N(1) distance is longer (2.172(5) Å) than that in Tc (2.150(4) Å) and in Rh (2.085(3) Å). In contrast to the technetium[18j] and rhodium (Figure 2), where the nitrogen atom of the uncoordinated pyridyl ring is located almost close to the P(1) atom, in ruthenium complex **3**, the uncoordinated pyridyl ring is located between two chlorine atoms (Figure 4) and the Cl(2)−Ru−Cl(3) angle (172.10(5)°) is smaller than those for Tc and Rh (173.36(5) and 173.40(4)°, respectively). The deviation of the coordinated pyridyl ring from the coordination plane is larger for the Ru compound. The displacements of M out of the plane $N_1C_1C_2C_3C_4C_5$ are 0.127 Å for Tc, 0.198(5) Å for Rh, and 0.640(7) Å for Ru compounds.

Compound **4**, the meridional isomer of well-known complex *fac*-[$RuCl_3$(DMSO-*S*)$_3$]$^-$,[24] was obtained from *cis*-$RuCl_2$(DMSO-*S*)$_3$(DMSO-*O*) and [NBu_4]Cl in a 1:1 mixture of CH_2Cl_2 and CH_3OH. As expected for the mer isomer, three Ru−Cl bands in the IR spectrum were observed (345, 334, and 297 cm^{-1}). Unlike the fac isomer (one ν(S═O) band at 1100 cm^{-1}), two ν(S═O) bands at 1105 and 1081 cm^{-1} were observed for **4**. The position of these bands indicate that all three DMSO ligands are coordinated through S. The ESI(−) MS spectrum of compound **4** shows the [$RuCl_3$(DMSO)$_3$]$^-$ ($m/z = 441$) and [$RuCl_3$(DMSO)$_2$]$^-$ ($m/z = 363$) ions.

The reaction of **4** with PPh_2py (Ru:P = 1:3) in an acetone solution leads to the substitution of DMSO and Cl ligands and the formation of complex [RuCl(PPh_2py-*P*,*N*)$_2$(PPh_2py-*P*)]Cl (**5**), which contains two chelating phosphine ligands. Complex **5** displays in the IR spectrum only one ν(Ru−Cl) band at 279 cm^{-1} and, characteristic for the chelate PPh_2py ligand, a ν(C═N) band at 1583 cm^{-1}. In the $^{31}P\{^1H\}$ NMR spectrum in acetone-d_6 solution, two signals were observed, a triplet centered at δ 53.05 and a doublet at δ −2.80 with intensity 1:2 and coupling constant 30.5 Hz. These data indicate that complex **5** has the mer structure, in which two P atoms in the trans position are part of chelating rings and a third P atom (cis to the trans P atoms) acts as a monodentate ligand. A compound with the same formula as **5** obtained by Faraone[18h] has the fac structure, in which one PPh_2py molecule is coordinated via a P atom while the remaining two act as chelating ligands. Its $^{31}P\{^1H\}$ NMR spectrum exhibits three signals at δ 47.31 (dd, ^2J(PP) 33.6 and 27.7 Hz), −6.53 (dd, ^2J(PP) 33.6 and 27.7 Hz), and −7.72 (t, ^2J(PP) 27.7 Hz). The structural data for this compound were not given. Compound **5** in $CHCl_3$ solution is quickly converted into a fac isomer, as proved by $^{31}P\{^1H\}$ NMR.

(43) Medhi, O. K.; Agarwala, U. *Inorg. Chem.* **1980**, *19*, 1381.

Table 4. Selected Bond Lengths (Å) and Angles (deg) for *fac*-[RuCl(PPh$_2$py-*P*,*N*)$_2$(PPh$_2$py-*P*)]Cl (*fac*-**5**)

Ru−N(2)	2.118(5)	Ru−P(2)	2.3081(18)
Ru−N(3)	2.122(5)	Ru−P(1)	2.3220(17)
Ru−P(3)	2.2964(17)	Ru−Cl(1)	2.4218(16)
N(2)−Ru−N(3)	92.77(18)	P(3)−Ru−P(1)	100.15(7)
N(2)−Ru−P(3)	161.48(14)	P(2)−Ru−P(1)	101.74(6)
N(3)−Ru−P(3)	69.24(14)	N(2)−Ru−Cl(1)	88.52(13)
N(2)−Ru−P(2)	68.33(13)	N(3)−Ru−Cl(1)	83.87(13)
N(3)−Ru−P(2)	89.32(13)	P(3)−Ru−Cl(1)	93.68(6)
P(3)−Ru−P(2)	105.81(6)	P(2)−Ru−Cl(1)	155.55(6)
N(2)−Ru−P(1)	98.28(14)	P(1)−Ru−Cl(1)	88.87(6)
N(3)−Ru−P(1)	166.62(13)		

A solution of **5** in $CHCl_3$ layered with Et_2O gives crystals of *fac*-[RuCl(PPh$_2$py-*P*,*N*)$_2$(PPh$_2$py-*P*)]Cl (*fac*-**5**) suitable for X-ray analysis. Figure 5 shows a perspective view of the crystal structure of *fac*-**5**. The coordination geometry of the ruthenium atom is octahedral with very large distortions caused mainly by the small bite angles of the two chelating ligands (see Table 5). The coordination sphere in *fac*-**5** is similar to that found for *cis*,*cis*-[RuCl$_2$(PPh$_2$py-*P*,*N*)$_2$] (**6**)[18h] by Faraone et al. Both complexes *fac*-**5** and **6** have N−Ru−P bite angles for two chelating ligands markedly smaller than 90° (68,33(13) and 69.24(14)° for *fac*-**5**; 68.7(3) and 69.6(3)° for **6**). In complex *fac*-**5**, analogous to the case of compound **6**, the two pyridine rings coordinated to ruthenium are arranged orthogonally around the metal center. The Ru−Cl bond length of 2.4218(16) Å is comparable to the ruthenium−chlorine bond reported for **6** (2.420(3) Å) and for *cis*,*cis*-[RuCl$_2$(CO)$_2$(PPh$_2$py-PN)][18g] (2.417(2) Å). The ruthenium−nitrogen bond lengths are the same (2.118(5) Å) in *fac*-**5** and very similar to that observed in **6** (2.13(1), 2.063(8) Å). The Ru−P bond lengths are equal to 2.2963(17), 2.3077(18), and 2.3218(17) Å. The longest Ru−P value is for the nonchelated phosphine in the trans position to the nitrogen atom; the two remaining values are slightly longer than the corresponding distances observed in **6** (2.265(4), 2.270(3) Å). The two intermolecular weak hydrogen bonds linking C52−H52···Cl8 and C53−H53···Cl8 atoms of two molecules of chloroform and the Cl^- anion are observed (D···A distances are 3.310(8) and 3.341(10) Å; D−H···A angles are 166 and 165° for C52 and C53, respectively).

Structural and Spectroscopic Correlation between Complexes with Chelating Coordinated PPh$_2$py-*P*,*N* Ligands. Crystallographic and $^{31}P\{^1H\}$ NMR data for all known metal complexes with one or two P−N chelates are given in Tables 5 and 6. The literature reports on the PPh$_2$py ligand acting as a P−N chelate are rather scarce. Four-membered chelate rings are very strained, and small P−M−N bite angles are expected. An increase of the P−M−N angle in complexes with one (63.2−70.68°) and two (64.13−71.26°) chelating ligands is observed. The extent of the compression of the chelate angle follows the order W > Re > Tc > Ru ≈ Rh > Pt and W > Ru ≈ Rh > Fe in compounds with one and two P−N ligands, respectively. It is also seen from Tables 5 and 6 that the shortening of the M−N and M−P bond lengths followed in the same direction. This trend shows the effect of the relative size of the coordinating metal on the bite angle and bond lengths. Furthermore, it was found that the symmetric deformation

Table 5. Comparison of Structural and ^{31}P NMR Data for Metal Complexes with One Chelating PPh$_2$py-*P*,*N* Ligand[a]

M	complex	S4′ [b] (deg)	P−M−N (deg)	M−N (Å)	M−P$_{CH}$ (Å)	L[c]	δ(P$_{CH}$)[d]	ref
W	[W(CO)$_4$(PN)]	10.1	63.2	2.256	2.543	CO	−11	18b
	[W(CO)$_2$NO(PN)(P)]$^+$	12.21	64.49	2.240	2.537	CO	−18.3	18m
Re	[ReCl$_3$O(PN)]	1.9	63.57	2.280	2.423	Cl		18e
Tc	[TcCl$_2$(NO)(PN)(P)]	17.29	66.09	2.198	2.400	Cl		18f
	[TcCl$_3$(PN)(P)]	18.02	66.36	2.150	2.4554	Cl		18j
Ru	[RuCl$_3$(PN)(P)]	17.32	66.63	2.1171	2.415	Cl		TW
	[Ru(cymene)Cl(PN)]$^+$	3.88	67.47	2.104	2.3311	aren	−11.72	18d
		4.34	67.26	2.106	2.332		−17.4	18n
	[Ru(bipy)$_2$(PN)]$^{2+}$	6.1	68.37	2.092	2.3038	N_{py}	43.86	18o
	[C$_6$Me$_6$RuCl(PN)]$^+$	8.39	67.72	2.107	2.412	aren	−11.25	18c
	[RuCl$_2$(CO)$_2$(PN)]	8.47	68.678	2.119	2.321	Cl	−6.84	18g
	[RuCl$_2$(dppb)(PN)]	32.6	68.0	2.146	2.348	Cl	−20.9	18a
Rh	[RhCp*Cl(PN)]$^+$	7.7	67.3	2.132	2.338	Cp*	−11.6	18k
	[RhCl$_3$(PN)(P)]	18.20	69.116	2.083	2.322	Cl	−31.97	TW
Pt	[PtCl(PN)(P)]	2.86	70.76	2.07	2.223	Cl	−50.3	18l
	[PtCH$_3$(PN)(P)]$^+$	17.6	70.68	2.07	2.327	CH$_3$	−17.6	6g

[a] (PN) = chelating PPh$_2$py-*PN*, (P) = terminal coordinated PPh$_2$py-*P*, TW = this work. [b] Angular symmetric deformation coordinate S4′,[44] defined as the sum of the M−P−C angles minus the sum of the C−P−C angles. [c] Ligand trans to P$_{CH}$. [d] δ(P$_{CH}$) is a ^{31}P chemical shift for a chelating phosphine.

Table 6. Comparison of Structural and ^{31}P NMR Data for Metal Complexes with Two Chelating PPh$_2$py-*P*,*N* Ligands[a]

M	complex	S4′ [b] (deg)	P−M−N (deg)	M−N (Å)	M−P$_{CH}$ (Å)	L[c]	δ(P$_{CH}$)[d]	ref
W	[W(CO)(NO)(PN)$_2$]$^+$	11.6	64.13	2.210	2.556	CO	2.3	18m
		15.38	65.50	2.258	2.449	N_{py}	−12.8	
Ru	[RuCl$_2$(PN)$_2$]	16.33	69.57	2.063	2.270	N_{py}	2.64	18h
		21.69	68,65	2.13	2.265	Cl	−4.49	
	[RuCl(PN)$_2$(P)]$^+$	22.6	69.26	2.122	2.2964	N_{py}	−6.53	TW
		24.39	68.34	2.119	2.3077	Cl	−7.72	18h
Rh	[RhCl$_2$(PN)$_2$]$^+$	4.51	68.86	2.149	2.2731	N_{py}	−15.1	TW
Fe	[Fe(CO)$_2$(PN)$_2$]$^{2+}$	−8.49	69.72	2.004	2.345	CO		18i
		3.56	71.26	2.015	2.253	N_{py}		

[a] (PN) = chelating PPh$_2$py-*P*,*N*, (P) = terminal coordinated PPh$_2$py-*P*, TW = this work. [b] Angular symmetric deformation coordinate S4′,[44] defined as the sum of the M−P−C angles minus the sum of the C−P−C angles. [c] Ligand trans to P$_{CH}$. [d] δ(P$_{CH}$) is a ^{31}P chemical shift for a chelating phosphine.

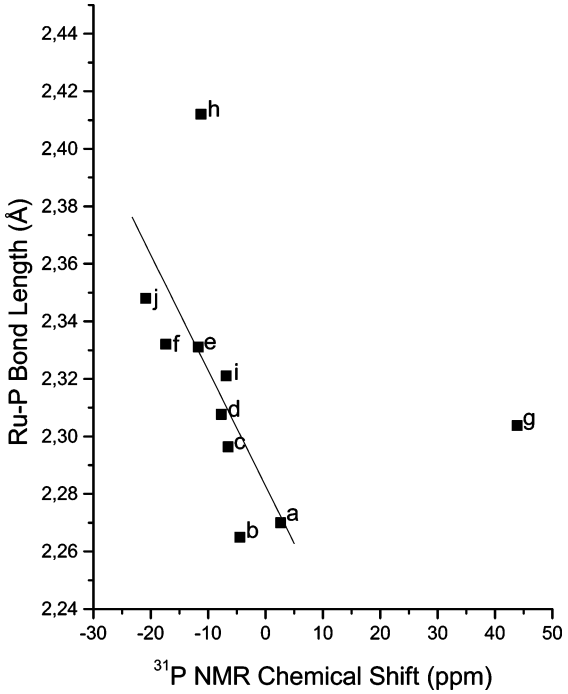

Figure 6. Graph of Ru−P bond length (Å) vs $^{31}P\{^1H\}$ NMR chemical shift (ppm) for a series of ruthenium(II) complexes containing PPh_2py-*P,N*. (a and b) *cis*-$[RuCl_2(PPh_2py\text{-}P,N)_2]$,[18h] (c and d) *fac*-$[RuCl(PPh_2py\text{-}P,N)_2(PPh_2py\text{-}P)]^+$,[18h] (e) $[Ru(cymene)Cl(PPh_2py\text{-}P,N)]^+$,[18d] (f) $[Ru(cymene)Cl(PPh_2py\text{-}P,N)]^+$,[18n] (g) $[Ru(bipy)_2(PPh_2py\text{-}P,N)]^{2+}$,[18o] (h) $[C_6Me_6RuCl(PPh_2py\text{-}P,N)]^+$;[18c] (i) *cis, cis*-$[RuCl_2(CO)_2(PPh_2py\text{-}P,N)]$;[18g] (j) $[RuCl_2(dppb)(PPh_2py\text{-}P,N)]$.[18a] $^{31}P\{^1H\}$ NMR data in $CDCl_3$ (a−f, h, j), CD_2Cl_2 (i), and CD_3CN (g).

coordinates S4′ [44] depend on the trans influence of ligands occupying trans-to-P coordination sites and on the M−N bond length. The mean S4′ values are small, and phosphine ligands are considerably flattened in complexes with CO, arene, and N_{py} ligands. The smallest S4′ value (−8.49°) was found in the $[Fe(CO)_2(Pph_2py\text{-}P,N)_2]^{2+}$ compound with CO trans to P and the smallest M−N bond length value (2.004 Å).[18i]

A plot of the Ru−P bond lengths for Ru(II)(PPh_2py-*P,N*)-containing complexes versus their $^{31}P\{^1H\}$ chemical shift data is shown in Figure 6. It is interesting that, as for Ru(II) complexes with triphenylphosphine and 1,4-bis(diphenylphosphino)butane (dppb),[45] complexes with PPh_2py chelating ligands show a pronounced negative correlation between $^{31}P\{^1H\}$ chemical shift and Ru−P bond length. The negative slope (−0.0040 Å ppm^{-1}) of the line drawn in Figure 6 is very similar to that of the plot for PPh_3 and dppb systems (−0.0029 Å ppm^{-1}), whereas the intercept (2.2828 Å) is substantially different from that for the PPh_3 (2.465 Å) and dppb (2.423Å) systems.[45] The explanation of this fact seems rather simple. It is well-known that the $^{31}P\{^1H\}$ chemical shift for phosphine ligands depends on the C−P−C angle.[33] When the C−P−C angle opens, the ^{31}P NMR shift moves to a lower field. This is true when phosphine is monodentate or part of a five-or-more-membered chelating ligand, but in the case of four-membered chelating phosphines, the C−P−C increase and $^{31}P\{^1H\}$ chemical shift moves to a higher field. Thus changes in the ^{31}P chemical shifts in comparison with the data for monodentate coordination provide a good diagnostic tool for identifying the mode of coordination of PPh_2py ligands. It is also seen from Figure 6 that in the case of $[Ru(bipy)_2(PPh_2py\text{-}P,N)]^{2+}$, the chemical shift is much higher than expected (43.86 ppm).[18o] This is most probably caused by transformation in solution of the chelating phosphine into a monohapto ligand coordinated only via a P atom. The correlation between structural and spectroscopic parameters for PPh_2py-*P,N* could be expected for the complexes of other metals, but there are not yet sufficient experimental data to discuss this dependence.

Acknowledgment. This work was supported by the KBN (Committee of Scientific Research), Grant 4 T09A 00224.

Supporting Information Available: Crystallographic data files of **1**, **2**, **3**, and *fac*-**5** in CIF format. This material is available free of charge via the Internet at http://pubs.acs.org.

IC051442K

(44) Dunne, B. J.; Morris, R. B.; Orpen, A. G *J. Chem. Soc., Dalton Trans.* **1991**, 653.

(45) (a) Jessop, P. G.; Rettig, S. J.; Lee, C.-L.; James, B. R. *Inorg. Chem.* **1991**, *30*, 4617. (b) MacFarlane, K. S.; Joshi, A. M.; Rettig, S. J.; James, B. R. *Inorg. Chem.* **1996**, *35*, 7304. (c) Queiroz, S. L.; Batista, A. A.; Oliva, G.; Gambardella, M. T.; Santos, R. H. A.; MacFarlane, K. S.; Rettig, S. J.; James, B. R. *Inorg. Chim. Acta* **1998**, *267*, 209.